Universiteit Leiden
The Netherlands

Design of a rotating disk electrode setup operating under high pressure and temperature: application to CO2 reduction on gold

Marques da Silva, A.H.M.; Vos, R.E.; Schrama, R.J.C.; Koper, M.T.M.

Citation
Marques da Silva, A. H. M., Vos, R. E., Schrama, R. J. C., & Koper, M. T. M. (2024). Design of a rotating disk electrode setup operating under high pressure and temperature: application to CO2 reduction on gold. *Electrochimica Acta*, *489*. doi:10.1016/j.electacta.2024.144612

Version:	Publisher's Version
License:	Creative Commons CC BY 4.0 license
Downloaded from:	https://hdl.handle.net/1887/3768871

Note: To cite this publication please use the final published version (if applicable).

Electrochimica Acta 498 (2024) 144612

Contents lists available at ScienceDirect

Electrochimica Acta

journal homepage: www.journals.elsevier.com/electrochimica-acta

Design of a Rotating Disk Electrode setup operating under high pressure and temperature: Application to CO_2 reduction on gold

Alisson H.M. da Silva [a], Rafaël E. Vos [a], Robin J.C. Schrama [b], Marc T.M. Koper [a,*]

[a] Leiden Institute of Chemistry, Leiden University, Leiden 2300 RA, the Netherlands
[b] Leiden Institute of Physics, Fine Mechanical Department, Leiden University, Leiden 2300 RA, the Netherlands

ARTICLE INFO

Keywords:
Rotating disk electrode
High pressure
High temperature
Cell design
CO_2 reduction

ABSTRACT

We describe the design and development of a rotating disk electrode (RDE) cell capable of operating at pressures up to 200 bar and temperatures up to 200 °C. This setup enables electrochemical surface characterization through techniques such as voltammetry and impedance spectroscopy, under different mass transport regimes. Furthermore, evaluation of catalytic performance, including CO_2 reduction, is possible as the system works in a semi-continuous mode interfaced with online gas sample measurements. As a proof of concept of the high-pressure cell designed, we examined the temperature-dependent changes in the cyclic voltammograms (CVs) of polycrystalline gold up to 150 °C and 50 bar. Additionally, online catalytic performance of CO_2 reduction to CO on a rotating polycrystalline gold disk electrode was investigated under different pressure and temperature. Our results indicate a positive impact of temperature on the faradaic efficiency (FE) towards CO up to 50 °C, beyond which a rapid drop in performance was observed at atmospheric pressure. Conversely, increasing pressure positively affected CO_2 solubility in the electrolyte, resulting in enhanced FE towards CO, reaching approximately 90 % at 6 bar compared to 40 % at atmospheric pressure. Notably, further increases in pressure did not significantly alter the FE, but led to higher current densities. Moreover, at pressures exceeding 6 bar, we observed a plateau in efficiency at temperatures higher than 50 °C. This observation suggests that increasing pressure can sustain CO_2 electrolysis, validating the hypothesis that increasing CO_2 solubility would suppress catalytic decay at higher temperatures. This study opens up promising avenues for future investigations in electrocatalysis, ranging from fundamental explorations of surface modifications induced by variations in temperature and pressure to the development of high-performance catalysts.

1. Introduction

The CO_2 electrochemical reduction reaction (CO_2RR) offers a promising strategy for CO_2 utilization when powered with renewable electricity. Through this approach, CO_2 can be converted using water as a proton donor, which provides an advantage compared to the use of H_2 in conventional thermal catalytic conversion. A wide range of products has already been reported from CO_2RR, including C_1 to C_3 compounds such as formic acid, CO, ethylene, ethanol, n-propanol, as well as other compounds like aldehydes and ketones [1,2]

To date, CO_2RR has primarily been studied under ambient conditions, where Cu is the sole metal capable of facilitating C—C coupling and thereby producing C_{2+} compounds with higher yields [3,4]. Conversely, in thermal catalysis, Cu-based catalysts predominantly yield C_1 compounds such as CO and methanol [5,6]. Fe and Co are well-established metals utilized in the Fischer-Tropsch reaction to generate olefins and high-density carbonaceous compounds at temperatures exceeding 200 °C and pressures of 30 bar [7–9]. However, Fe exhibits limited electrochemical CO_2 conversion capability [10,11]. Some of these disparities between thermal and electrocatalysis may be related to variations in reaction conditions, wherein temperature and pressure significantly influence compound adsorption on the catalytic surface. For example, Zhang et al. [12] demonstrated that the selectivity for multicarbon products follows a volcano trend based on the ratio of the Cu–CO stretching band to the Cu–CO rotation band. This ratio increases with increasing temperature [13], which agrees with the enhanced formation of C_{2+} compounds at temperatures around 50 °C compared to room temperature.

The temperature effect is typically not studied in CO_2RR studies and often avoided due to membrane instability and/or rapid catalyst

* Corresponding author.
E-mail address: m.koper@lic.leidenuniv.nl (M.T.M. Koper).

https://doi.org/10.1016/j.electacta.2024.144612
Received 13 March 2024; Received in revised form 17 June 2024; Accepted 18 June 2024
Available online 22 June 2024
0013-4686/© 2024 The Author(s). Published by Elsevier Ltd. This is an open access article under the CC BY license (http://creativecommons.org/licenses/by/4.0/).

deactivation at higher temperatures. However, in practical applications, electrolyzers will invariably operate at elevated temperatures [14–16]. Only a few studies delve into the temperature effect at the fundamental level. We have previously studied the temperature effect on the CO_2RR on Cu electrodes and its impact on product distribution [13], as well as the kinetic parameters of CO_2RR on Au electrodes at elevated temperatures [17]. Recently, a similar temperature dependence has been demonstrated for C_{2+} compounds in the CO reduction reaction using Cu gas diffusion electrodes (GDE) operating under more industrial conditions (current densities up to 500 mA/cm^2) [18]. These works show similar results: the catalytic performance towards $CO_{(2)}RR$ decreases at temperatures over 50 °C, favoring hydrogen evolution reaction (HER). The reasons for HER enhancement at the expense of $CO_{(2)}RR$ are attributed to a change in the hydrophobicity of the gas diffusion layer (GDL), leading to flooding of the GDE [18], reconfiguration of the catalyst particles at the atomic scale due to increased atom mobility at elevated temperatures [13,18], and CO_2 availability potentially becoming the limiting factor at higher temperatures [17]. However, if CO_2 availability were the limiting factor, an increase in CO_2 concentration, such as by raising the pressure, should prevent the observed decrease in performance in the formation of carbon products at temperatures exceeding 50 °C.

The impact of pressure on CO_2RR has been extensively studied in the literature [19–25]. At the end of the last century, Hara and coworkers made an important contribution identifying the pressure effect on CO_2 reduction [19,21,26,27]. They demonstrated that a 44 % faradaic efficiency to CO could be achieved on glassy carbon at 30 bar and approximately 100 mA/cm^2 [21], despite glassy carbon being known as an inert substrate with minimal activity for CO_2 conversion at atmospheric pressure [28]. Hara et al. [26]. also investigated the effect of pressure on several metal wires (Ti, Zr, Nb, Ta, Cr, Mo, W, Mn, Fe, Co, Rh, Ir, Ni, Pd, Pt, Cu, Ag, Au, Zn, Al, In, Sn, Pb, and Bi) at 167 mA/cm^2 and identified mainly CO and HCOOH as the primary carbon products at 30 bar for all metals, including Pt, where a 56 % FE was found for CO + HCOOH, whereas >90 % FE towards H_2 is expected at 1 bar. Additionally, Hara et al. [19] investigated the impact of pressure on the CO formation from CO_2 reduction using Co-, Cu-, Rh-, Ni-, Pd-, Ag-, and Ag-GDEs, with Ag showing the highest catalytic activity. Specifically, the FE to CO on Ag increased from around 40 % to 86 % by raising the pressure from 1 bar to 20 bar. Ramdin et al. [22,23] studied the effect of pressure on formic acid formation using a tin-based electrode. They explored different scenarios, including the use of cationic exchange membranes, bipolar membranes, and pH effects. In summary, they achieved an improvement in FE to formate from approximately 40 % to 90 % by increasing the pressure up to 50 bar. This enhancement was attributed to the higher concentration of CO_2 in solution. Recently, Zong et al. [24] have reviewed the influence of the pressure on CO_2RR. They concluded that pressure can influence catalytic performance through various mechanisms, such as the thermodynamics of the reaction, the acid/base buffer balance ($CO_2/HCO_3^-/CO_3^{2-}$), and the degree of coverage of CO_2 on the catalyst surface. Interestingly, metals such as Ni, Fe, and Pt exhibit low selectivity to CO at ambient conditions but demonstrate significant improvements in CO and/or formic acid production at relatively high CO_2 pressures [27,29,30], which aligns with the hypothesis that the disparities between thermal and electrocatalysis may be bridged by variations in reaction conditions.

However, to date, there are no studies that investigate the combined effects of mass transport, temperature, and pressure simultaneously at a fundamental level. One reason for this gap may be the complexity involved in designing and constructing an electrochemical cell capable of altering parameters such as temperature and pressure, as well as the fluid dynamics within the cell (e.g., by varying the rotation speed of the disk electrode), while ensuring safety and proper electrical connections. Additionally, the compartment housing the electrochemical components must be predominantly metal-free to minimize metal contamination in the experiments.

Here, we present the design of a rotating disk electrochemical cell, which is based on a commercial (Parr) rotating cylinder electrode (RCE) high-pressure reactor, with several modifications. The designed high-pressure and high-temperature electrochemical cell is capable of operating in a semi-continuous mode under pressures of up to 200 bar and temperatures of up to 200 °C, with a maximum rotation speed of 2500 rpm for the disk electrode. In this system, several fundamental electrochemical surface investigations, such as cyclic and linear-sweep voltammetry, impedance spectroscopy, and electrochemical frequency modulation, can be conducted under different pressure, temperature, and mass transfer conditions. Additionally, catalytic performance investigations including $CO_{(2)}RR$, HER, oxygen evolution reaction (OER), electro-organic oxidation, nitrogen reduction, etc., can be explored, as the cell is also interfaced with online gas chromatography (GC) and mass spectrometry. As a proof of concept, we investigate here the influence of temperature, pressure, and rotation speed on CO_2RR on a gold electrode, while also providing surface characterization of polycrystalline Pt and Au via cyclic voltammetry, to demonstrate cleanliness and reproducibility of the electrochemical experiments. Our results show that the combination of high pressure and high temperature favorably impact current density and Faradaic efficiency towards CO.

2. Methods

2.1. Chemicals

All solutions used in this work were made by dissolving appropriate amounts of chemicals in Milli-Q water (Millipore, resistivity ≥ 18.2 MΩ cm). All chemicals were used as received: $KHCO_3$ (>99.5 %, Sigma-Aldrich), $KMnO_4$ (ACS reagent, Fluka), H_2SO_4 (ACS Reagent, Fluka), H_2O_2 (35 %, Merck), CO_2 (Linde, 4.5), and Ar (Linde, 5.0).

2.2. General procedures

Prior to each day of experiments, all glassware, the PEEK cup, and the PEEK membrane separator were soaked in a 0.5 M H_2SO_4 and 1 g/L $KMnO_4$ acid solution for at least 12 h. The glassware and the PEEK compartments were then rinsed and submerged in a solution of H_2O_2 and H_2SO_4 to remove any remaining manganese oxide. Next, the solution was drained, and the glassware and the PEEK compartments were rinsed with ultrapure water and boiled three times in ultrapure water (≥18.2 MΩ cm).

In this work, a Au disk electrode embedded in a PEEK holder with dimensions of 8 mm diameter, Au wire (2 mm) or Pt wire (0.5 mm) exposing 5 cm^2 area were used as working electrodes. For the wires, a flame annealing procedure were used for surface cleaning and preparation. For gold disk electrode, gold was mechanically polished on a microcloth (Buehler) with diamond suspensions (Buehler) of 3.0, 1.0, and 0.25 μm successively. Next, the electrode was rinsed and sonicated in ultrapure water for at least 10 min to remove remnant diamond suspension from the surface.

2.3. High-pressure and high-temperature Rotating Disk Electrode (RDE) electrochemical cell

The electrochemical cell developed in this work is based on the Rotating Cylinder Electrode (RCE) high-pressure reactor developed by Parr Company, with several modifications. Fig. 1 shows a schematic of the high-pressure Rotating Disk Electrode (RDE) cell developed for this study. Pictures of the actual cell and its components are provided in Fig. S1. A 120 mL PEEK insert was positioned in the stainless-steel vessel (Fig. S1b and c). The electrolyte was placed within the PEEK insert, preventing contact with the metal wall of the vessel. Another PEEK compartment with a circular window of 25 mm diameter was positioned on top of the insert, creating an H-type cell configuration (Fig. S1 d-f). This configuration allows for the incorporation of a membrane that

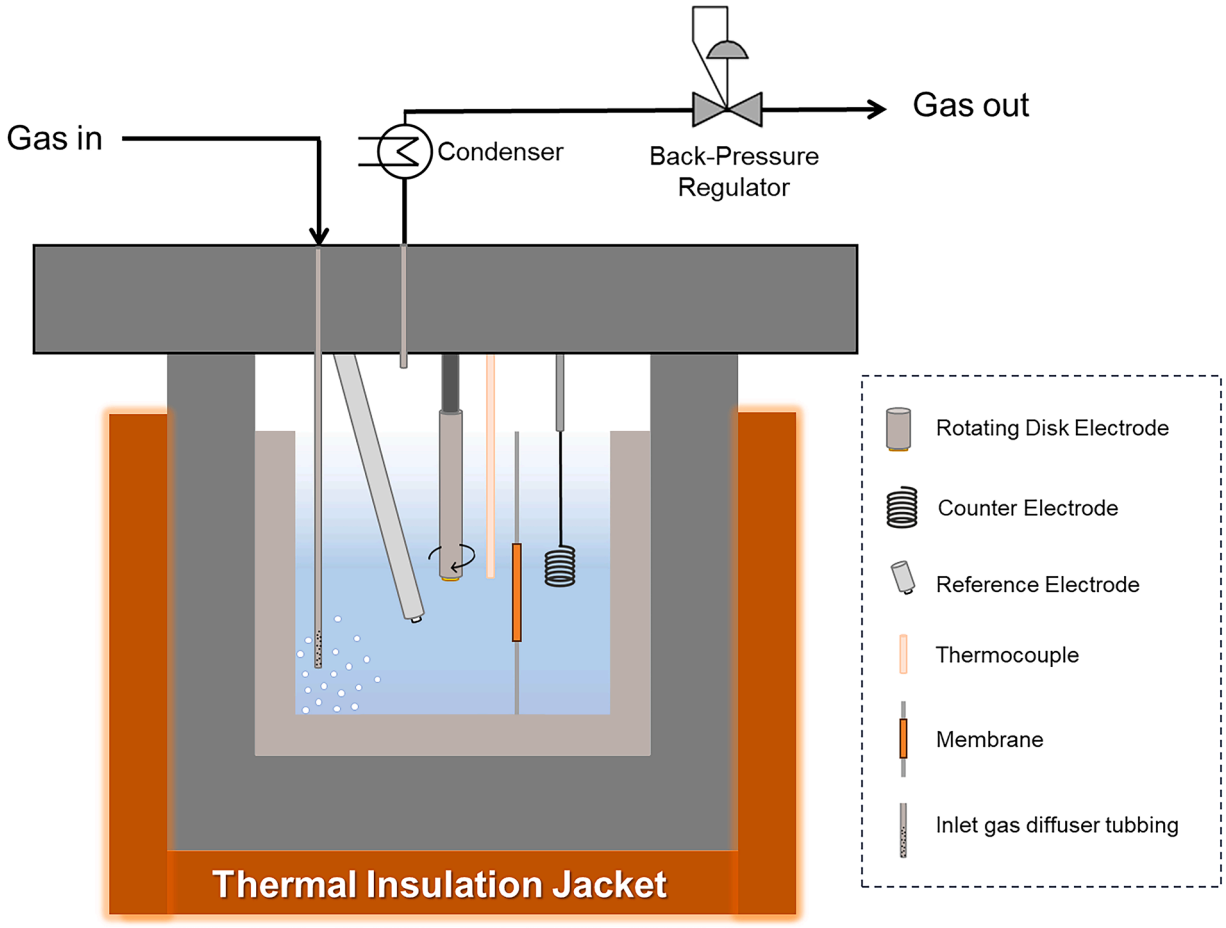

Fig. 1. Schematic illustration of the high-pressure and high-temperature rotating disk electrode cell.

separates the working electrode compartment from the counter electrode compartment. The working and counter electrode compartments can be filled with up to 90 mL and 10 mL of electrolyte, respectively.

The system can accommodate wire, cylinder, or disk electrode configurations for the working electrode. In this work, both wires and disk electrodes were used. The disk electrode was made of an 8 mm x 2 mm (diameter x height) cylinder embedded in PEEK material (Fig. S1f), exposing only the electrode disk area and preventing contact between the electrode sides and any other metal with the electrolyte. Wires offer flexibility and can be easily modified to achieve a desired exposed surface area. Furthermore, at high temperatures (>100 °C), disk electrodes embedded with a plastic matrix are compromised as the metal and plastic exhibit different thermal expansion characteristics, allowing electrolyte to permeate from the junction, compromising the measurements. In contrast, wires offer more flexibility at high temperatures.

A coated DSA titanium mesh was used as the counter electrode for CO_2 electrolysis tests, while Au (or Pt) wire was used as the counter electrode for CV characterization measurements. An UltraDeg® High-Pressure Ag/AgCl (Corr instruments) and a PiperION-A anionic exchange membrane (A40 from Versogen) were used as the reference electrode and membrane, respectively, for all tests. The metal walls of the reference, thermocouple, and holders were meticulously wrapped with Teflon tape to prevent metal exposure (Fig. S1h and i). Wrapping the thermocouple with Teflon tape requires more time for temperature stabilization, but it prevents metal contact in the electrolyte. Even the lid and other cell parts that do not directly contact the electrolyte were meticulously coated with Teflon and Kapton tape before the tests start to prevent condensed steam droplets from the metal vessel walls and contaminating the electrolyte, especially during high-temperature tests. A Teflon cylinder was placed on the top of the PEEK cup to decrease the headspace volume of the vessel (Fig. S1c and j).

An inlet PEEK gas diffuser tubing for continuously electrolyte saturation and a back-pressure regulator (BPR) are connected to the cell to operate the electrolysis reaction in a semi-continuous mode. A external thermal insulator jacked is placed around the vessel so that the temperature can be increased and isolated. A condenser is placed before the BPR to prevent steam and volatile compounds from being carried away. The system can operate at pressures up to 200 bar and temperatures up to 200 °C, although we limited our tests up to 50 bar and 150 °C. The pressure measured in the system is gauge pressure (barg) rather than absolute pressure (bar). At sea level, 0 barg corresponds to 1.01325 bar. Therefore, the pressures reported in this manuscript will be represented in barg rather than bar.

It is important to mention that for studies involving high current, the design of the cathode and anode chambers should be slightly modified to prevent the mixing of higher concentrations of O_2 and H_2 in the vessel at elevated temperatures. In such cases, the anode compartment should be a closed chamber with a small tubing leading to the outlet gas tube of the cell, passing through the condenser where O_2, in case of reduction reactions are studied on the working electrode, is released. This configuration ensures that O_2 and H_2 are mixed after exiting the hot chamber but before reaching the backpressure valve, thereby maintaining both the cathode and anode compartments at the same pressure. This is crucial to prevent a pressure gradient across the membrane. In the experiments conducted in this study, relatively low currents were employed, and either high CO_2 flow or Ar flow was utilized, resulting in less than 1 % of the total flow being a mixture of O_2 and H_2. As a result, the approach of mixing the gasses after the condenser was deemed

unnecessary.

2.4. Cyclic voltammograms of Au and Pt wires in different temperatures and pressures

Cyclic voltammograms (CVs) of Au and Pt wires were recorded in a 0.1 M H_2SO_4 electrolyte. Au or Pt wire was used as the counter-electrode for the Au or Pt working-electrodes, respectively. UltraDeg® High-Pressure Ag/AgCl (Corr Instruments) was used as the reference electrode. Before each measurement, the electrolyte was purged with argon at a flow rate of 100 mL/min for at least 30 min. The measurements were recorded with a scan rate of 100 mV/s using an Ivium potentiostat (Ivium Technologies) to control the potentials. For the CVs recorded while changing temperature and pressure, argon was continuously used as the purging gas.

2.5. Linear sweep voltammograms of rotating disk Au electrode at different pressures, temperature, and rotation speed

Linear sweep voltammograms (LSVs) of the rotating disk Au electrode were recorded following the procedure described for cyclic voltammograms, but in a 0.1 M $KHCO_3$ electrolyte and using a coated DSA titanium mesh as the counter electrode. For tests conducted in the presence of CO_2 (CO_2-saturated electrolyte), CO_2 was purged at a flow rate of 100 mL/min for at least 30 min before the measurements began. For tests conducted in the absence of CO_2, Ar-purging was carried out at the same flow rate and duration. The rotation speed was mechanically controlled by the high-pressure unit, ranging from 0 rpm to 2500 rpm.

For LSVs measurements in different pressures, the cell was submerged in a water bath to maintain a constant temperature in order to mitigate the effects of temperature fluctuations resulting from increased pressure.

2.6. CO_2 reduction in the RDE high-pressure and high-temperature cell

0.1 M CO_2-saturated $KHCO_3$ (pH = 6.8) was used as the electrolyte for CO_2RR. In all experiments, the electrolyte was continuously purged with the corresponding gas (CO_2 or Ar) at a rate of 100 mL/min using high-pressure mass flow controllers from Brooker. All potentials were controlled with an Ivium potentiostat (Ivium technologies). Resistances were determined via impedance spectroscopy (EIS) and 85 % ohmic drop compensation was applied during the experiment. Gas samples were analyzed every 10 min using gas chromatography (Micro-GC, Agilent), equipped with two thermal conductivity detectors (TCD). One TCD used a CP-SIL 5B column to separate CO_2, CH_4, and C_2H_4, while the other TCD used a combination of MS5A and CP-PORABOND Q columns to separate H_2, O_2, N_2, CH_4, and CO.

3. Results and discussion

3.1. Au and Pt CVs

Voltammograms of Au and Pt wires in 0.1 M H_2SO_4 were recorded in the designed cell (Fig. 1) and compared to their established and well-known profiles to demonstrate that the cell functions as intended. Fig. S2a-b shows the CV of Au and Pt wires, respectively, where all the features align with a conventional and clean voltammogram of a polycrystalline surface [31–34]. The CVs were measured until 300 cycles were completed (Fig. S2c-d), and it can be observed that the CVs exhibit the same features with a slight surface roughening after 300 cycles were completed.

The effect of pressure on the blank CV was evaluated on the Au wire. CVs were recorded as the cell pressure was changed from 0 barg to 50 barg in 0.1 M H_2SO_4 purged with argon as an inert gas (Fig. 2). Before the pressure was increased, argon was purged into the electrolyte for at least 30 min while the potential was held at 0.2 V. There is no noticeable change in the CV after the cell pressure was increased from 0 barg to 50 barg, indicating that pressure does not affect the oxidation and reduction on the Au surface. This result is expected, as the increase in pressure primarily enhances gas dissolution in the electrolyte (and minimal liquid compression), and it is not expected that argon would influence the gold surface features. The pressure in the vessel is raised by an argon flow

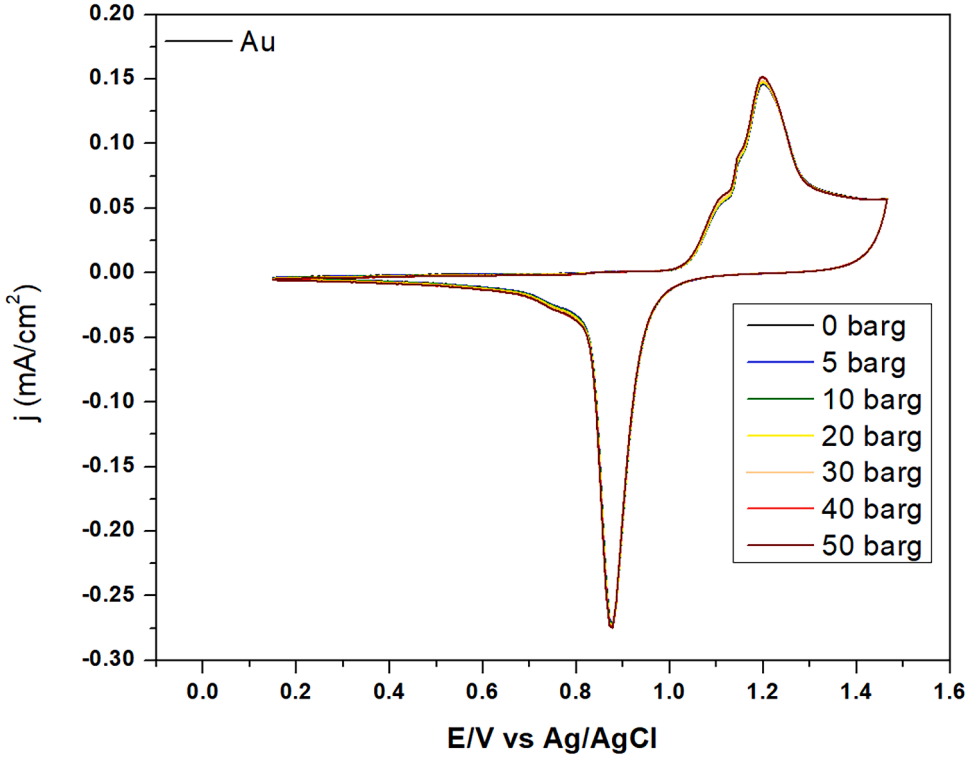

Fig. 2. Cyclic voltammograms at different pressures on Au, using scan rate of 100 mV/s, in 0.1 M H_2SO_4 and at 22 °C.

rate of 150 mL min^{-1}, taking approximately 2 h to increase from 0 barg to 50 barg. Consequently, we can also rule out the possibility that time (during this 2-h test) affects the CV profile.

Temperature, on the other hand, can significantly alter the blank CVs of the electrodes since the kinetics of oxidation and reduction should be strongly temperature dependent, in addition to small changes in the corresponding thermodynamic redox potentials with temperature. To prevent electrolyte evaporation, Au CVs were recorded under a pressure of 30 barg at different temperatures and the results are shown in Fig. 3. At this pressure, the boiling point of water exceeds 200 °C, which guarantees the liquid phase with a reasonable safe margin for the tests shown in Fig. 3. Notably, Fig. 3a reveals that both the reduction and oxidation peaks shift positively and negatively, respectively, with increasing temperature, demonstrating enhanced reversibility and peak sharpness. For instance, the reduction and oxidation peaks at 0.87 V and 1.20 V at 30 °C, shift to 0.98 V and 1.12 V at 100 °C, respectively (Fig. 3b). As illustrated in Fig. 3, the designed cell facilitates the evaluation of surface changes under high-pressure and high-temperature conditions. However, it is important to mention that caution must be taken when working at elevated temperatures using Ag/AgCl reference electrodes. As depicted in Fig. S3 and further detailed in Note S1, Cl^- species may leak from the high-pressure reference electrode at temperatures exceeding 100 °C, potentially leading to surface electrodissolution and compromising measurement accuracy. This can be prevented by storing the reference not in saturated KCl, but in a 0.1 M KCl solution. Additionally, we have evaluated the use of a high-pressure PdH reference electrode (Cormet Testing System), which does not contain any anion species. Therefore, we are able to get Cl^--free measurements but this reference electrode is highly sensitive to O_2. Consequently, this sensitivity limits measurements to very low currents, as O_2 can be produced in situ at the counter electrode. If the objective is solely focused on catalytic performance studies of the entire cell, the system can also be easily utilized without a reference electrode, and chronopotentiometry tests can be conducted while only recording cell voltage.

3.2. CO_2 reduction on Au at different temperatures and pressures using RDE mode

Next, the CO_2 reduction reaction on Au in an RDE mode was evaluated at higher pressures and moderate temperatures. The aim was to demonstrate that the designed cell is suitable for studies involving the impact of different parameters such as mass transport, temperature, and pressure on CO_2 reduction under well-defined conditions. Fig. 4a illustrates the effect of rotation speed on the linear sweep voltammogram of CO_2-saturated 0.1 M $KHCO_3$ electrolyte at 0 barg and room temperature. Mass transfer coefficients can be calculated from the Levich equation [35]. However, detailed understanding of mass transport is highly complicated, as pH gradients exist, which are also mass transport dependent [36] and, therefore, they will not be calculated here. Goyal et al. [37] demonstrated that an increase in rotation speed of a disk Au electrode leads to a decrease in the overall current density in a CO_2-saturated $NaHCO_3$ electrolyte, the opposite observed in Fig. 4a. This decrease was attributed to the inhibition of HER caused by the reduction in local alkalinity near the electrode surface, thereby suppressing HER related to water reduction. However, this behavior was observed primarily at low current densities (up to 3.5 mA/cm^2), while other factors such as bubble formation and release become prevalent at higher current densities. We observe a similar behavior at lower current densities as shown in Fig. S5 and briefly described in Note 2 in the Supporting Information. Therefore, we attribute the enhancement in the overall current, more pronounced at current densities above 15 mA/cm^2, to the improved bubble removal facilitated by the higher rotation speed.

The impact of temperature on the CO_2RR and HER was investigated in a CO_2-saturated $KHCO_3$ electrolyte while maintaining constant rotation speed (750 rpm) and pressure (5 barg). Fig. 4b reveals a pronounced effect of temperature on the overall current density. For instance, the current density of around −70 mA/cm^2 at −1.8 V and 22 °C increased by around −200 mA/cm^2 at 65 °C. However, CO_2 solubility generally decreases with increasing temperature, negatively impacting the CO_2RR rate. Detangling the specific influence of temperature on CO_2RR and HER solely from Fig. 4b is not possible. Nevertheless, previous work by Vos et al., [13] and Schellekens et al. [18]. demonstrates that at ambient pressures, temperatures around 50 °C can favor the production of multi-carbon products, such as ethylene, on Cu electrodes. Therefore, while increasing temperature might adversely affect CO_2 conversion due to decreased CO_2 solubility, it can simultaneously play a significant role by modifying catalytic rates and/or changing adsorption modes, potentially leading to a more selective product spectrum.

Fig. 5a-d illustrate the effect of pressure at a constant rotation rate of 750 rpm at room temperature. Fig. 5a demonstrates the CO_2 pressure effect on the overall current when using a CO_2-saturated $KHCO_3$ electrolyte. Notably, the current density at −1.5 V increases roughly 5-fold as pressure rises from 0 barg to 50 barg. It has been reported that CO_2 solubility in water as a function of pressure has a logarithmic dependence [38–41], as also shown in Fig. S6a. However, at pressures below 50 bar, CO_2 solubility increases linearly with a rate of 0.0099 mol_{CO2}/L

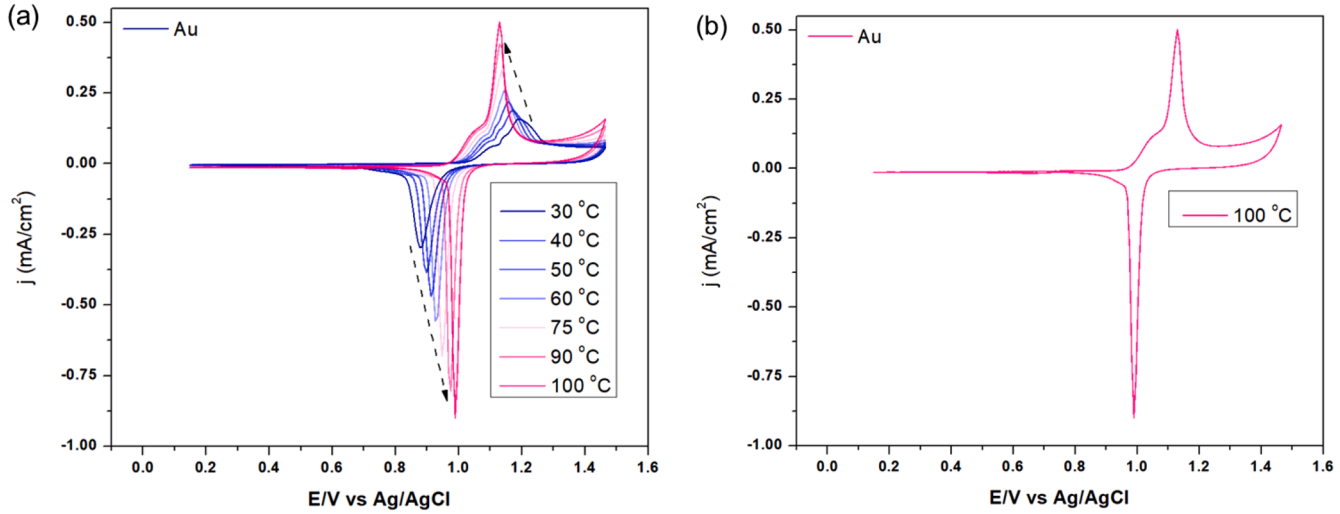

Fig. 3. Cyclic voltammograms in 0.1 M H_2SO_4 at different temperatures: (a) from 30 °C to 100 °C and (b) at 100 °C;.

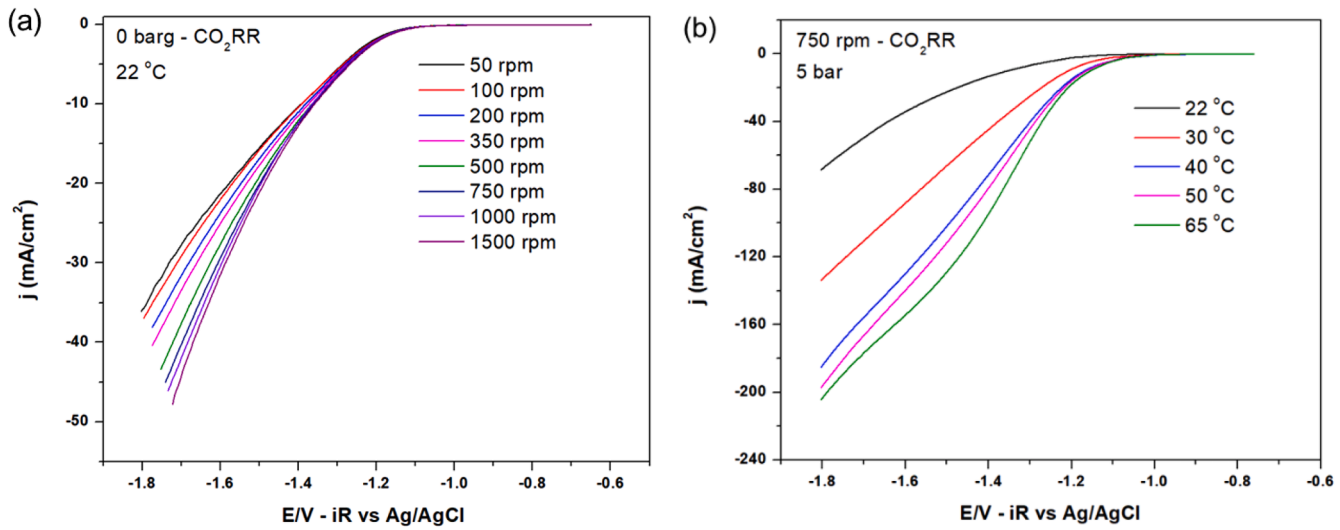

Fig. 4. Linear sweep voltammograms (LSVs) in 0.1 M $KHCO_3$ at (a) different scan rate recorded at 0 barg and 22 °C; and (b) different temperatures recorded at 5 barg and 750 rpm.

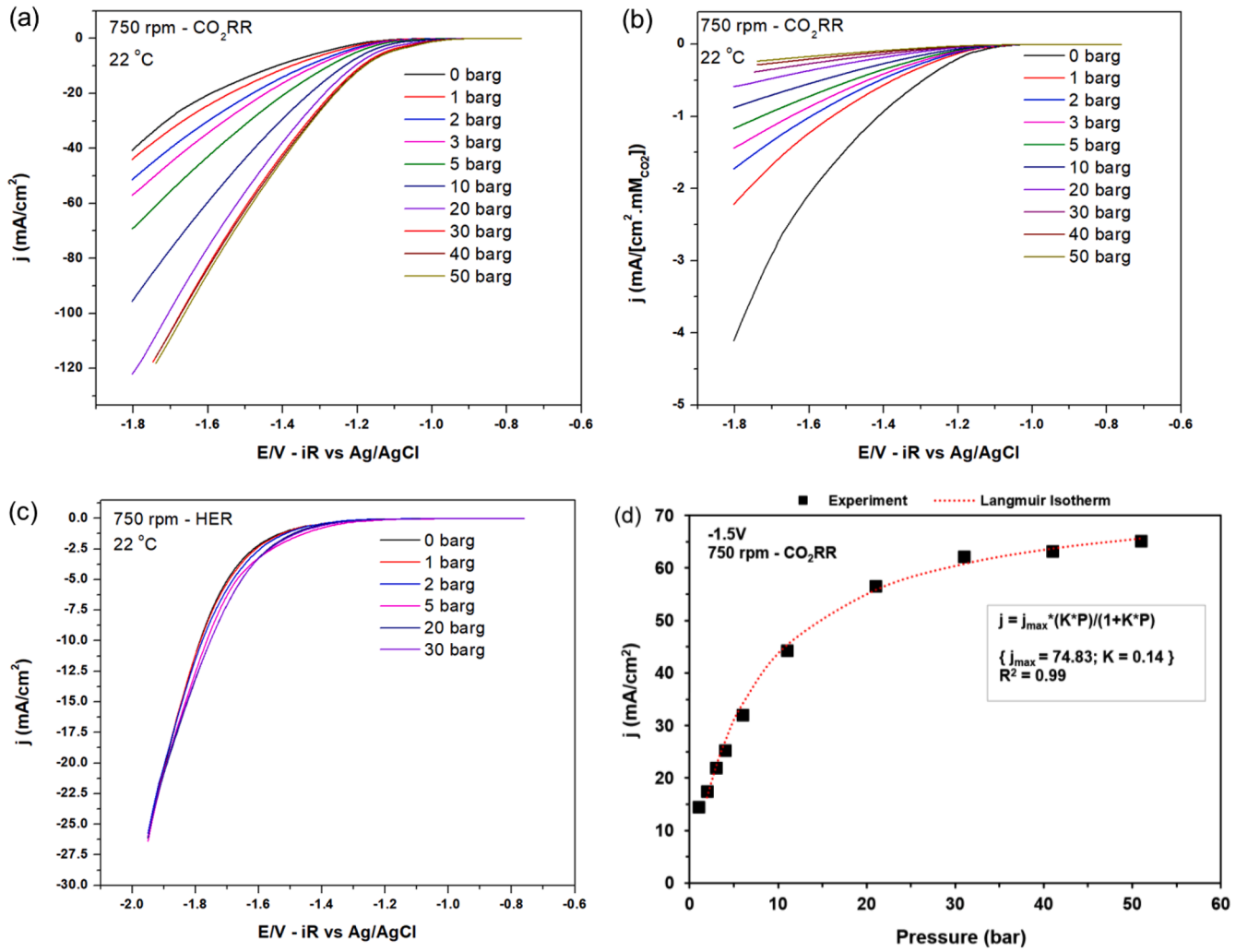

Fig. 5. (a) LSVs recorded in CO_2-saturated electrolyte at different pressures under 22 °C and 750 rpm; (b) LSVs recorded in CO_2-saturated electrolyte at 750 rpm and 22 °C, but normalized by the CO_2 concentration; (c) LSVs recorded in Ar-saturated electrolyte at 750 rpm and 22 °C; and (d) Langmuir isotherm fitting at −1.5 V and 750 rpm using $j = j_{max} * (K * P)/(1 + K * P)$ equation.

per bar increase, as shown in Fig. S6b. Despite the linear rise in CO_2 concentration from 1 to 50 bar, no corresponding linear increase in current density is observed. Fig. 5b illustrates the impact of pressure on the overall current density normalized by the CO_2 concentration at that pressure (based on data from Duan et al. [38] and Fig. S6b). The normalized current density exhibits a significant decrease from 0 barg to 50 barg. This indicates that the reaction order in CO_2 is smaller than 1. We hypothesize that the increase in CO_2 concentration might partially inhibit the competitive HER by the adsorption of either CO_2 or CO onto the gold electrode, which could also explain the overall decrease in the normalized current density. Fig. 5c support this hypothesis. In an Ar-saturated electrolyte, in which only HER takes place, the pressure minimally affects the overall current, indicating that the observed pressure effect in Fig. 5a and b is primarily due to the CO_2 concentration. Furthermore, Fig. 5d shows the total current density as function of CO_2 pressure at −1.5 V, which resembles a Langmuir isotherm, indicating that the current density is related with CO_2 pressure through an adsorption process. Specifically, by fitting the experimental data with $j = j_{max}.(K*P)/(1+K*P)$ Langmuir equation, where K is the adsorption coefficient, P is pressure, and j is the current density, we achieved a fitting with an R^2 value of 0.99. Therefore, the overall current density over pressure seems to be directly related to the CO_2 (or CO) adsorption. This would explain why the increase in current density levels off at higher pressures, as CO_2 adsorption cannot increase infinitely. Furthermore, it indicates that HER can be inhibited by increasing the CO_2 pressure as the increased CO_2 (or CO) coverage leaves less active sites for HER. Moreover, Fig. S7 suggests reversibility of the effect of CO_2 pressure as the current density returns to its initial range when the CO_2 pressure is reduced from 50 barg back to 0 barg. This observation further supports the hypothesis that the overall current density is primarily influenced by the CO_2 concentration in the electrolyte.

To evaluate the impact of temperature and pressure on the selectivity, gaseous products were measured using gas chromatography during 3 h electrolysis at constant potential. This is possible in our cell design as it is a system which can operate in semi-continuous mode, where CO_2 is continuously bubbled into electrolyte and out of the high pressure cell. This makes it possible to connect the cell to an online gas chromatograph to detect H_2 and CO. We have previously shown that this rotation speed has a positive effect on the CO formation on a gold electrode due to the inhibition of the HER [37]. This inhibition results from the decrease in local alkalinity near the electrode surface with enhanced mass transport. The same effect is expected at higher pressures; therefore, all tests were carried out at a constant rotation speed of 750 rpm. Fig. 6a shows the impact of temperature on the FE to CO at 0 barg and 750 rpm. No liquid products were identified by liquid chromatography within the detection limit. H_2 was the sole byproduct

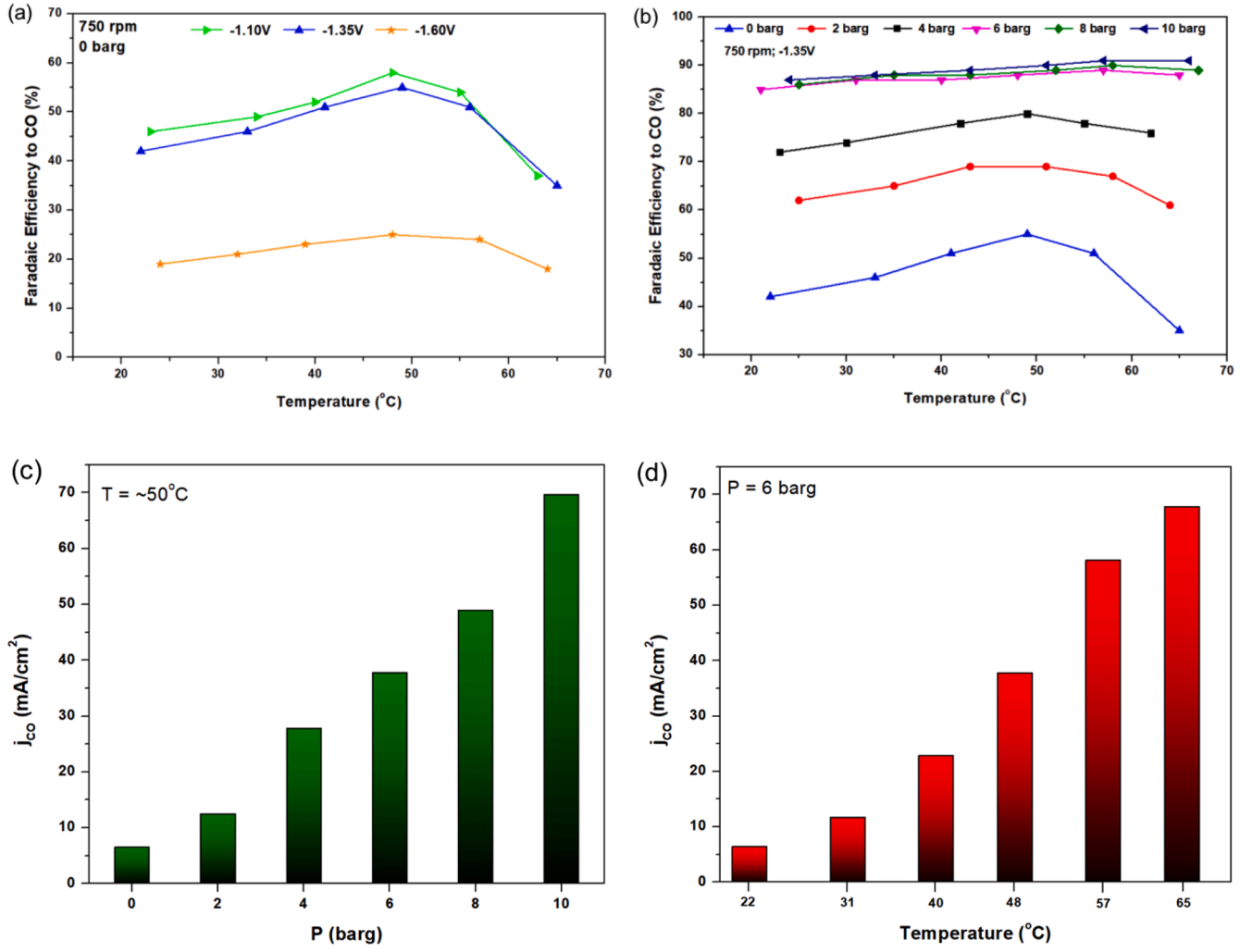

Fig. 6. (a) Faradaic efficiency to CO in different temperature at −1.1 V, −1.35 V, and −1.6 V under 0 barg and rotation speed of 750 rpm.(b) CO_2 reduction at different temperatures and pressures with constant potential of −1.35 V and constant rotation speed of 750 rpm; (c) recorded current densities towards CO at different pressures at constant potential of −1.35 V and constant rotation speed of 750 rpm at 50 °C; and (d) recorded current densities towards CO at different temperatures at constant potential of −1.35 V and constant rotation speed of 750 rpm at 6 barg.

detected, alongside CO from the CO_2RR process. As a general trend, for all evaluated potentials, the FE for CO slightly increases from room temperature to 50 °C before decreasing again at temperatures exceeding 50 °C. H_2, on the other hand, follows the opposite direction. This result is consistent with our earlier findings [17], in which an optimal temperature of 55 °C for CO_2 conversion to CO on a gold electrode was observed, followed by a decrease at higher temperatures, attributed to the decreasing solubility of CO_2 at elevated temperatures, thereby favoring HER over CO_2RR. The initial increase of the FE towards CO with increasing temperature was ascribed to the differences in kinetics, as CO_2RR shows higher apparent activation energy and therefore the activity of CO_2RR increases faster with temperature than the HER activity. In that work, we concluded that an increase in CO_2 solubility would likely extend the optimal temperature for CO_2 reduction. If the observed decrease is indeed primarily linked to CO_2 availability, increasing pressure could mitigate this decline at temperatures exceeding 50 °C, as the concentration of CO_2 would increase accordingly. Fig. 6b illustrates the influence of temperature and pressure on the FE to CO at 750 rpm and −1.35 V. No liquid products were detected within the detection limit of the liquid chromatography, with H_2 as the sole byproduct from CO_2RR. Remarkably, the FE for CO increases from 42 % at room temperature to 62 % at 2 barg and approximately 86 % at pressures exceeding 6 barg. At pressures exceeding 6 barg, there are minimal changes in FE with variations in temperature, although the partial current density for CO increases with pressure (Fig. 6c). Interestingly, the effect of temperature on the FE decreases by increasing the pressure. This may be due to the fact that even at room temperature the FE is already high, leaving less room for improvement at elevated temperatures. Another interesting observation is that the decline at temperatures exceeding 50 °C is significantly mitigated by increasing pressure, confirming that CO_2 availability is a critical factor in suppressing HER at higher temperatures. It also corroborates our hypothesis raised in relation with Fig. 5, where higher CO_2 concentration might partially inhibit the competitive HER, explaining the lower the current density normalized by the CO_2 concentration in different pressures. Thus, elevated pressures increase the FE towards CO and make the effect of temperature on the FE insignificant. However, temperature has still a positive effect on the current density towards CO as shown in Fig. 6d. At the constant pressure of 6 barg, the current density increases one order of magnitude by increasing the temperature from room temperature to 65 °C, with no negative impact in the FE to CO (~90 %). Therefore, Fig. 6 demonstrates the substantial impact of pressure and temperature on catalytic performance towards CO. When pressure and temperature are combined, there is potential to simultaneously enhance the FE and the overall current density, thereby providing opportunities for future studies on materials that are more active and selective for CO_2RR.

The CO_2RR at high pressure has been shown to exhibit an enhancement towards CO compared to atmospheric pressure. On similar electrode surfaces (polished flat surfaces), FE towards CO reaches approximately 80 % under optimal conditions of potential, rotation speed, temperature, and electrolyte [17,37,42,43]. In this study, an FE of 90 % was achieved at pressures exceeding 6 bar. This value could potentially be improved through further optimization. For instance, nanostructured gold electrodes, which have demonstrated >90 % FE towards CO at atmospheric pressure [44], could be a promising class of materials to investigate at high pressure and temperature for enhanced current density and stability. Cu electrodes, capable of producing more valuable compounds such as ethylene, ethanol, and n-propanol, have not yet been comprehensively explored in terms of their fundamental aspects under both high pressure and temperature. There are numerous opportunities for further investigation in this direction. Additionally, different classes of metals, typically inactive for CO_2RR, may become active under high pressure and temperature conditions. Hara et al. [26] have already indicated this possibility. For instance, Fe electrodes, which exhibit low activity towards CO_2RR, demonstrated an FE of 40 % towards formic acid under high pressure. If similar investigations are conducted under high temperature, "electrochemical Fisher-Tropsch" type reactions could potentially be discovered. Finally, we recently reported the impact of bubbles on HER [45,46], and expect that bubble dynamics will be pressure and temperature dependent. Such studies will be possible using the system presented in this work.

4. Conclusions

The impact of pressure, temperature, and mass transport on the CO_2 reduction on Au electrodes was successfully investigated using a high-pressure and high-temperature rotating disk electrode electrochemical cell. This system offers the opportunity for fundamental surface characterization without apparent metal contamination, as demonstrated by 300 reproducible cycles of the well-known blank voltammetry of polycrystalline Pt and Au in 0.1 M H_2SO_4. Additionally, we examined how Au cyclic voltammograms are affected by increasing temperature and pressure up to 150 °C and 50 bar, although Cl^- leakage from Ag/AgCl reference electrode may occur when operating at high temperatures. The system operates in a semi-continuous mode, with CO_2 (or any other gas) continuously bubbling into the electrolyte, and can be easily connected to an online gas chromatograph and mass spectrometry for investigating CO_2 reduction at different pressures and temperatures on the rotating disk electrode. Linear sweep voltammograms of CO_2RR on the Au electrode indicated that current densities were positively influenced by increasing rotation speed, temperature, and pressure. The total current density follows a Langmuir dependence on CO_2 concentration explaining the smaller pressure effect at the highest pressures and suggesting that CO_2 or CO adsorption may block active sites for the competing HER. Electrolysis experiments show that elevated pressure can inhibit the effect of temperature on the CO efficiency, but both pressure and temperature can significantly increase the current density towards CO. This result suggests that increasing both pressure and temperature allows for sustained CO_2 electrolysis at high activities outcompeting HER.

This work suggests several promising avenues for future investigations. On a fundamental level, voltammetry techniques can be employed to explore the surface changes on the electrode induced by variations in temperature and pressure. From a catalysis viewpoint, the designed high-pressure and high-temperature cell presents a platform for discovering novel catalysts for $CO_{(2)}RR$. As demonstrated here, using a gold electrode, these parameters dramatically enhance catalytic performance. Similar improvements are expected for Cu electrodes leading to the formation of more valuable C_{2+} products. As commented in the introduction, altering temperature and pressure pushes the electrochemical system towards the well-known thermochemical regime. Consequently, it is expected that previously inactive materials at ambient conditions might become active under temperature and/or pressure, leading to the discovery of new material classes for electrochemical conversion. Moreover, the system can be easily extended to investigations beyond CO_2 conversion, offering prospects for electrooxidation studies, nitrogen-based reactions, and organic electrosynthesis.

CRediT authorship contribution statement

Alisson H.M. da Silva: Writing – review & editing, Writing – original draft, Methodology, Investigation, Formal analysis, Data curation, Conceptualization. **Rafaël E. Vos:** Writing – review & editing, Methodology, Investigation, Formal analysis, Data curation. **Robin J.C. Schrama:** Methodology. **Marc T.M. Koper:** Writing – review & editing, Supervision, Funding acquisition, Formal analysis, Conceptualization.

Declaration of competing interest

The authors declare that they have no known competing financial interests or personal relationships that could have appeared to influence

the work reported in this paper.

Data availability

Data will be made available on request.

Acknowledgments

This research was carried out under project number ENPPS. IPP.019.002 in the framework of the Research Program of the Materials innovation institute (M2i) (www.m2i.nl) and received funding from Tata Steel Nederland Technology BV and the Dutch Research Council (NWO) in the framework of the ENW PPP Fund for the top sectors and from the Ministry of Economic Affairs in the framework of the "PPS-Toeslagregeling".

Supplementary materials

Supplementary material associated with this article can be found, in the online version, at doi:10.1016/j.electacta.2024.144612.

References

[1] A.H.M. da Silva, G. Karaiskakis, R.E. Vos, M.T.M. Koper, Mechanistic insights into the formation of hydroxyacetone, acetone, and 1,2-propanediol from electrochemical CO $_2$ reduction on copper, J. Am. Chem. Soc. 145 (2023) 15343–15352, https://doi.org/10.1021/jacs.3c03045.

[2] K.P. Kuhl, E.R. Cave, D.N. Abram, T.F. Jaramillo, New insights into the electrochemical reduction of carbon dioxide on metallic copper surfaces, Energy Environ. Sci. 5 (2012) 7050, https://doi.org/10.1039/c2ee21234j.

[3] Y. Hori, A. Murata, R. Takahashi, Formation of hydrocarbons in the electrochemical reduction of carbon dioxide at a copper electrode in aqueous solution, J. Chem. Soc. Faraday Trans. 1 85 (1989) 2309, https://doi.org/10.1039/f19898502309. Physical Chemistry in Condensed Phases.

[4] Y. Hori, A. Murata, R. Takahashi, S. Suzuki, Enhanced formation of ethylene and alcohols at ambient temperature and pressure in electrochemical reduction of carbon dioxide at a copper electrode, J. Chem. Soc. Chem. Commun. 17 (1988), https://doi.org/10.1039/c39880000017.

[5] J. Niu, H. Liu, Y. Jin, B. Fan, W. Qi, J. Ran, Comprehensive review of Cu-based CO2 hydrogenation to CH3OH: insights from experimental work and theoretical analysis, Int. J. Hydrogen Energy 47 (2022) 9183–9200, https://doi.org/10.1016/j.ijhydene.2022.01.021.

[6] Y.F. Shi, S. Ma, Z.P. Liu, Copper-based catalysts for CO $_2$ hydrogenation: a perspective on active sites, EES Catal. 1 (2023) 921–933, https://doi.org/10.1039/D3EY00152K.

[7] Z. Gholami, F. Gholami, Z. Tišler, J. Hubáček, M. Tomas, M. Bačiak, M. Vakili, Production of light Olefins via Fischer-Tropsch process using iron-based catalysts: a review, Catalysts 12 (2022) 174, https://doi.org/10.3390/catal12020174.

[8] B.H. Davis, Fischer−Tropsch synthesis: comparison of performances of iron and cobalt catalysts, Ind. Eng. Chem. Res. 46 (2007) 8938–8945, https://doi.org/10.1021/ie0712434.

[9] Z. Gholami, Z. Tišler, V. Rubáš, Recent advances in Fischer-Tropsch synthesis using cobalt-based catalysts: a review on supports, promoters, and reactors, Catal. Rev. 63 (2021) 512–595, https://doi.org/10.1080/01614940.2020.1762367.

[10] S. Nitopi, E. Bertheussen, S.B. Scott, X. Liu, A.K. Engstfeld, S. Horch, B. Seger, I.E. L. Stephens, K. Chan, C. Hahn, J.K. Nørskov, T.F. Jaramillo, I. Chorkendorff, Progress and perspectives of electrochemical CO $_2$ reduction on copper in aqueous electrolyte, Chem. Rev. 119 (2019) 7610–7672, https://doi.org/10.1021/acs.chemrev.8b00705.

[11] Y. Hori, Electrochemical CO2 Reduction on Metal Electrodes. Modern Aspects of Electrochemistry, Springer New York, New York, NY, 2008, pp. 89–189, https://doi.org/10.1007/978-0-387-49489-0_3.

[12] C. Zhan, F. Dattila, C. Rettenmaier, A. Bergmann, S. Kühl, R. García-Muelas, N. López, B.R. Cuenya, Revealing the CO Coverage-Driven C–C coupling mechanism for electrochemical CO $_2$ reduction on Cu $_2$ O nanocubes *via operando* Raman spectroscopy, ACS Catal. 11 (2021) 7694–7701, https://doi.org/10.1021/acscatal.1c01478.

[13] R.E. Vos, K.E. Kolmeijer, T.S. Jacobs, W. van der Stam, B.M. Weckhuysen, M.T. M. Koper, How temperature affects the selectivity of the electrochemical CO $_2$ reduction on copper, ACS Catal. 13 (2023) 8080–8091, https://doi.org/10.1021/acscatal.3c00706.

[14] D. Corral, J.T. Feaster, S. Sobhani, J.R. DeOtte, D.U. Lee, A.A. Wong, J. Hamilton, V.A. Beck, A. Sarkar, C. Hahn, T.F. Jaramillo, S.E. Baker, E.B. Duoss, Advanced manufacturing for electrosynthesis of fuels and chemicals from CO $_2$, Energy Environ. Sci. 14 (2021) 3064–3074, https://doi.org/10.1039/D0EE03679J.

[15] H.P. Iglesias van Montfort, T. Burdyny, Mapping spatial and temporal electrochemical activity of water and CO $_2$ electrolysis on gas-diffusion electrodes using infrared thermography, ACS Energy Lett. 7 (2022) 2410–2419, https://doi.org/10.1021/acsenergylett.2c00984.

[16] P. Lobaccaro, M.R. Singh, E.L. Clark, Y. Kwon, A.T. Bell, J.W. Ager, Effects of temperature and gas–liquid mass transfer on the operation of small electrochemical cells for the quantitative evaluation of CO $_2$ reduction electrocatalysts, Phys. Chem. Chem. Phys. 18 (2016) 26777–26785, https://doi.org/10.1039/C6CP05287H.

[17] R.E. Vos, M.T.M. Koper, The effect of temperature on the cation-promoted electrochemical CO $_2$ reduction on gold, ChemElectroChem. 9 (2022), https://doi.org/10.1002/celc.202200239.

[18] M.P. Schellekens, S.J. Raaijman, M.T.M. Koper, P.J. Corbett, Temperature-dependent selectivity for CO electroreduction on copper-based gas-diffusion electrodes at high current densities, Chem. Eng. J. 483 (2024) 149105, https://doi.org/10.1016/j.cej.2024.149105.

[19] K. Hara, T. Sakata, Large current density CO2 reduction under high pressure using gas diffusion electrodes, Bull. Chem. Soc. Jpn. 70 (1997) 571–576, https://doi.org/10.1246/bcsj.70.571.

[20] A.R.T. Morrison, N. Girichandran, Q. Wols, R. Kortlever, Design of an elevated pressure electrochemical flow cell for CO2 reduction, J. Appl. Electrochem. 53 (2023) 2321–2330, https://doi.org/10.1007/s10800-023-01927-7.

[21] K. Hara, A. Kudo, T. Sakata, Electrochemical CO2 reduction on a glassy carbon electrode under high pressure, J. Electroanal. Chem. 421 (1997) 1–4, https://doi.org/10.1016/S0022-0728(96)01028-5.

[22] M. Ramdin, A.R.T. Morrison, M. de Groen, R. van Haperen, R. de Kler, E. Irtem, A. T. Laitinen, L.J.P. van den Broeke, T. Breugelmans, J.P.M. Trusler, W. de Jong, T.J. H. Vlugt, High-pressure electrochemical reduction of CO $_2$ to formic acid/formate: effect of pH on the downstream separation process and economics, Ind. Eng. Chem. Res. 58 (2019) 22718–22740, https://doi.org/10.1021/acs.iecr.9b03970.

[23] M. Ramdin, A.R.T. Morrison, M. de Groen, R. van Haperen, R. de Kler, L.J.P. van den Broeke, J.P.M. Trusler, W. de Jong, T.J.H. Vlugt, High pressure electrochemical reduction of CO $_2$ to formic acid/formate: a comparison between bipolar membranes and cation exchange membranes, Ind. Eng. Chem. Res. 58 (2019) 1834–1847, https://doi.org/10.1021/acs.iecr.8b04944.

[24] S. Zong, A. Chen, M. Wiśniewski, L. Macheli, L.L. Jewell, D. Hildebrandt, X. Liu, Effect of temperature and pressure on electrochemical CO2 reduction: a mini review, Carbon Capture Sci. Technol. 8 (2023) 100133, https://doi.org/10.1016/j.ccst.2023.100133.

[25] L. Huang, G. Gao, C. Yang, X.-Y. Li, R.K. Miao, Y. Xue, K. Xie, P. Ou, C.T. Yavuz, Y. Han, G. Magnotti, D. Sinton, E.H. Sargent, X. Lu, Pressure dependence in aqueous-based electrochemical CO2 reduction, Nat. Commun. 14 (2023) 2958, https://doi.org/10.1038/s41467-023-38775-0.

[26] K. Hara, A. Kudo, T. Sakata, Electrochemical reduction of carbon dioxide under high pressure on various electrodes in an aqueous electrolyte, J. Electroanal. Chem. 391 (1995) 141–147, https://doi.org/10.1016/0022-0728(95)03935-A.

[27] K. Hara, A. Tsuneto, A. Kudo, T. Sakata, Change in the product selectivity for the electrochemical CO2 reduction by adsorption of sulfide ion on metal electrodes, J. Electroanal. Chem. 434 (1997) 239–243, https://doi.org/10.1016/S0022-0728(97)00045-4.

[28] J.A. Costamagna, M. Isaacs, M.J. Aguirre, G. Ramírez, I. Azocar, Electroreduction of CO2 catalyzed by metallomacrocyclics. N4-Macrocyclic Metal Complexes, Springer New York, New York, NY, 2006, pp. 191–254, https://doi.org/10.1007/978-0-387-28430-9_5.

[29] S. Huo, J. Lu, X. Wang, Electrodeposition of Ni on MWNTs as a promising catalyst for CO $_2$ RR, Energy Sci. Eng. 9 (2021) 1042–1047, https://doi.org/10.1002/ese3.889.

[30] X. Wei, S. Wei, S. Cao, Y. Hu, S. Zhou, S. Liu, Z. Wang, X. Lu, Cu acting as Fe activity promoter in dual-atom Cu/Fe-NC catalyst in CO2RR to C1 products, Appl. Surf. Sci. 564 (2021) 150423, https://doi.org/10.1016/j.apsusc.2021.150423.

[31] C. Jeyabharathi, P. Ahrens, U. Hasse, F. Scholz, Identification of low-index crystal planes of polycrystalline gold on the basis of electrochemical oxide layer formation, J. Solid State Electrochem. 20 (2016) 3025–3031, https://doi.org/10.1007/s10008-016-3228-1.

[32] P. Daubinger, J. Kieninger, T. Unmüssig, G.A. Urban, Electrochemical characteristics of nanostructured platinum electrodes – a cyclic voltammetry study, Phys. Chem. Chem. Phys. 16 (2014) 8392–8399, https://doi.org/10.1039/C4CP00342J.

[33] M.C.O. Monteiro, M.T.M. Koper, Alumina contamination through polishing and its effect on hydrogen evolution on gold electrodes, Electrochim. Acta 325 (2019) 134915, https://doi.org/10.1016/j.electacta.2019.134915.

[34] L. Jacobse, S.J. Raaijman, M.T.M. Koper, The reactivity of platinum microelectrodes, Phys. Chem. Chem. Phys. 18 (2016) 28451–28457, https://doi.org/10.1039/C6CP05361K.

[35] A.J. Bard, L.R. Faulkner, Electrochemical Methods: Fundamentals and Applications, 2nd ed., Wiley, New York, 2000.

[36] X. Liu, M.C.O. Monteiro, M.T.M. Koper, Interfacial pH measurements during CO $_2$ reduction on gold using a rotating ring-disk electrode, Phys. Chem. Chem. Phys. 25 (2023) 2897–2906, https://doi.org/10.1039/D2CP05515E.

[37] A. Goyal, G. Marcandalli, V.A. Mints, M.T.M. Koper, Competition between CO $_2$ reduction and hydrogen evolution on a gold electrode under well-defined mass transport conditions, J. Am. Chem. Soc. 142 (2020) 4154–4161, https://doi.org/10.1021/jacs.9b10061.

[38] Z. Duan, R. Sun, An improved model calculating CO2 solubility in pure water and aqueous NaCl solutions from 273 to 533 K and from 0 to 2000 bar, Chem. Geol. 193 (2003) 257–271, https://doi.org/10.1016/S0009-2541(02)00263-2.

[39] A. Hemmati-Sarapardeh, M.N. Amar, M.R. Soltanian, Z. Dai, X. Zhang, Modeling CO $_2$ solubility in water at high pressure and temperature conditions, Energy Fuels 34 (2020) 4761–4776, https://doi.org/10.1021/acs.energyfuels.0c00114.

[40] P. Zhang, S. Ren, Y. Shan, L. Zhang, Y. Liu, L. Huang, S. Pei, Enhanced stability and high temperature-tolerance of CO $_2$ foam based on a long-chain viscoelastic surfactant for CO $_2$ foam flooding, RSC Adv. 9 (2019) 8672–8683, https://doi.org/10.1039/C9RA00237E.

[41] Z. Khoshraftar, A. Ghaemi, Prediction of CO2 solubility in water at high pressure and temperature via deep learning and response surface methodology, Case Stud. Chem. Environ. Eng. 7 (2023) 100338, https://doi.org/10.1016/j.cscee.2023.100338.

[42] G. Marcandalli, A. Goyal, M.T.M. Koper, Electrolyte effects on the faradaic efficiency of CO $_2$ reduction to CO on a gold electrode, ACS Catal. 11 (2021) 4936–4945, https://doi.org/10.1021/acscatal.1c00272.

[43] H. Noda, S. Ikeda, A. Yamamoto, H. Einaga, K. Ito, Kinetics of electrochemical reduction of carbon dioxide on a gold electrode in phosphate buffer solutions, Bull. Chem. Soc. Jpn. 68 (1995) 1889–1895, https://doi.org/10.1246/bcsj.68.1889.

[44] S. Zhao, R. Jin, R. Jin, Opportunities and challenges in CO $_2$ reduction by gold- and silver-based electrocatalysts: from bulk metals to nanoparticles and atomically precise nanoclusters, ACS. Energy Lett. 3 (2018) 452–462, https://doi.org/10.1021/acsenergylett.7b01104.

[45] S. Park, D. Lohse, D. Krug, M.T.M. Koper, Electrolyte design for the manipulation of gas bubble detachment during hydrogen evolution reaction, Electrochim. Acta 485 (2024) 144084, https://doi.org/10.1016/j.electacta.2024.144084.

[46] S. Park, L. Liu, Ç. Demirkır, O. van der Heijden, D. Lohse, D. Krug, M.T.M. Koper, Solutal Marangoni effect determines bubble dynamics during electrocatalytic hydrogen evolution, Nat. Chem. 15 (2023) 1532–1540, https://doi.org/10.1038/s41557-023-01294-y.